NASA/TM—2014–217501

Multiphysics Modeling of an Annular Linear Induction Pump With Applications to Space Nuclear Power Systems

J. Kilbane and K.A.Polzin
Marshall Space Flight Center, Huntsville, Alabama

March 2014

The NASA STI Program…in Profile

Since its founding, NASA has been dedicated to the advancement of aeronautics and space science. The NASA Scientific and Technical Information (STI) Program Office plays a key part in helping NASA maintain this important role.

The NASA STI Program Office is operated by Langley Research Center, the lead center for NASA's scientific and technical information. The NASA STI Program Office provides access to the NASA STI Database, the largest collection of aeronautical and space science STI in the world. The Program Office is also NASA's institutional mechanism for disseminating the results of its research and development activities. These results are published by NASA in the NASA STI Report Series, which includes the following report types:

- TECHNICAL PUBLICATION. Reports of completed research or a major significant phase of research that present the results of NASA programs and include extensive data or theoretical analysis. Includes compilations of significant scientific and technical data and information deemed to be of continuing reference value. NASA's counterpart of peer-reviewed formal professional papers but has less stringent limitations on manuscript length and extent of graphic presentations.

- TECHNICAL MEMORANDUM. Scientific and technical findings that are preliminary or of specialized interest, e.g., quick release reports, working papers, and bibliographies that contain minimal annotation. Does not contain extensive analysis.

- CONTRACTOR REPORT. Scientific and technical findings by NASA-sponsored contractors and grantees.

- CONFERENCE PUBLICATION. Collected papers from scientific and technical conferences, symposia, seminars, or other meetings sponsored or cosponsored by NASA.

- SPECIAL PUBLICATION. Scientific, technical, or historical information from NASA programs, projects, and mission, often concerned with subjects having substantial public interest.

- TECHNICAL TRANSLATION. English-language translations of foreign scientific and technical material pertinent to NASA's mission.

Specialized services that complement the STI Program Office's diverse offerings include creating custom thesauri, building customized databases, organizing and publishing research results…even providing videos.

For more information about the NASA STI Program Office, see the following:

- Access the NASA STI program home page at <http://www.sti.nasa.gov>

- E-mail your question via the Internet to <help@sti.nasa.gov>

- Phone the NASA STI Help Desk at 757–864–9658

- Write to:
  NASA STI Information Desk
  Mail Stop 148
  NASA Langley Research Center
  Hampton, VA 23681–2199, USA

NASA/TM—2014–217501

Multiphysics Modeling of an Annular Linear Induction Pump With Applications to Space Nuclear Power Systems

J. Kilbane and K.A. Polzin
Marshall Space Flight Center, Huntsville, Alabama

National Aeronautics and
Space Administration

Marshall Space Flight Center • Huntsville, Alabama 35812

March 2014

Acknowledgments

The authors wish to thank Walter Frei from COMSOL for providing very helpful technical support. Additionally, the authors want to thank Jim Knox of Marshall Space Flight Center (MSFC) for working to address COMSOL license server issues. Continuing management support of this work by Jim Martin and J. Boise Pearson is appreciated, as well as the technical editing help provided by Anita Beatty during the assembly of this Technical Memorandum. J. Kilbane was supported through the Summer 2013 MSFC Propulsion Academy program.

Available from:

NASA STI Information Desk
Mail Stop 148
NASA Langley Research Center
Hampton, VA 23681–2199, USA
757–864–9658

This report is also available in electronic form at
<http://www.sti.nasa.gov>

TABLE OF CONTENTS

LIST OF FIGURES

LIST OF TABLES

LIST OF ACRONYMS AND SYMBOLS

AC	alternating current
ALIP	annular linear induction pump
ATC	ALIP test circuit
CFD	computational fluid dynamics
DC	direct current
EMF	electromotive force
FSP	fission surface power
MTCD	multiturn coil domain
NaK	sodium-potassium
TDU	technology demonstration unit
TM	Technical Memorandum

NOMENCLATURE

B	magnetic field density
B_r	radial component of magnetic field density
H	magnetic field strength
P_{IN}	electrical input power
V	voltage
Δp	increase in pressure across the pump
δ	skin depth
η	pump efficiency
μ	magnetic permeability
$\dot{v}$	volumetric flow rate
σ	electrical conductivity
ω	angular frequency of current

TECHNICAL MEMORANDUM

MULTIPHYSICS MODELING OF AN ANNULAR LINEAR INDUCTION PUMP WITH APPLICATIONS TO SPACE NUCLEAR POWER SYSTEMS

1. INTRODUCTION

Fission surface power (FSP) systems, which are capable of providing consistent performance at any location, could be used to generate power on the surface of the Moon, Mars, other planets and moons of our solar system, or on various near-Earth objects. This includes those areas near planetary poles or in other permanently shaded regions, offering the capability to provide on-demand power at any time, even at long distances from the Sun. Fission-based systems also offer the potential for outposts, crew, and science instruments to operate in a power-rich environment while maintaining a relatively small footprint for the reactor system. NASA has been exploring technologies with the goal of reducing the cost and technical risk of employing FSP systems. A reference 40-kW_e option has been devised that is cost competitive with alternatives while providing more power for less mass anywhere on the lunar surface.[1–4] The reference FSP system is also readily extensible for use on Mars. On Mars, the system would be capable of operating through global dust storms and providing year-round power at any Martian latitude.

One key technology associated with the reference FSP system is the pump that circulates liquid-metal coolant through the reactor system. The pump must be compatible with the liquid sodium-potassium (NaK) coolant and have adequate performance to enable a viable flight system. Presently, this task is accomplished in the reference design using an annular linear induction pump (ALIP), which circulates the reactor coolant without the use of moving components. Two separate pumps were recently fabricated and shipped to NASA Marshall Space Flight Center where they were tested in a dedicated apparatus designed to quantify pump performance (the ALIP test circuit, or ATC). Pump efficiencies in these tests were in the 5%–6% range,[5,6] underperforming expectations. An effort has been initiated to develop a flexible multiphysics model that accurately represents an ALIP to provide a better understanding of the performance scaling and develop design strategies that can help increase performance in later iterations. This Technical Memorandum (TM) provides a present view of the state of this modeling effort. For the sake of completeness, note that a similar multiphysics ALIP modeling effort was recently presented by Goldsteins et al.[7] and general ALIP design optimization work has been presented by Maidana et al.[8]

2. REVIEW OF ANNULAR LINEAR INDUCTION PUMP EXPERIMENTAL TESTING

The ATC apparatus, shown schematically in figure 1, was fabricated to allow for performance testing of liquid-metal induction pumps. The system and testing results are described in detail in references 5 and 6. The pressure produced by the pump (Δp) is measured using two absolute pressure transducers located at the downstream and upstream ends of the pump, while the volumetric flow rate ($\dot{v}$) is measured using a calibrated liquid-metal electromagnetic flowmeter. A wattmeter provides a measure of the real input power to the pump (P_{IN}), permitting the calculation of pump efficiency as

$$\eta = (\dot{v}\Delta p) / P_{IN} \quad . \tag{1}$$

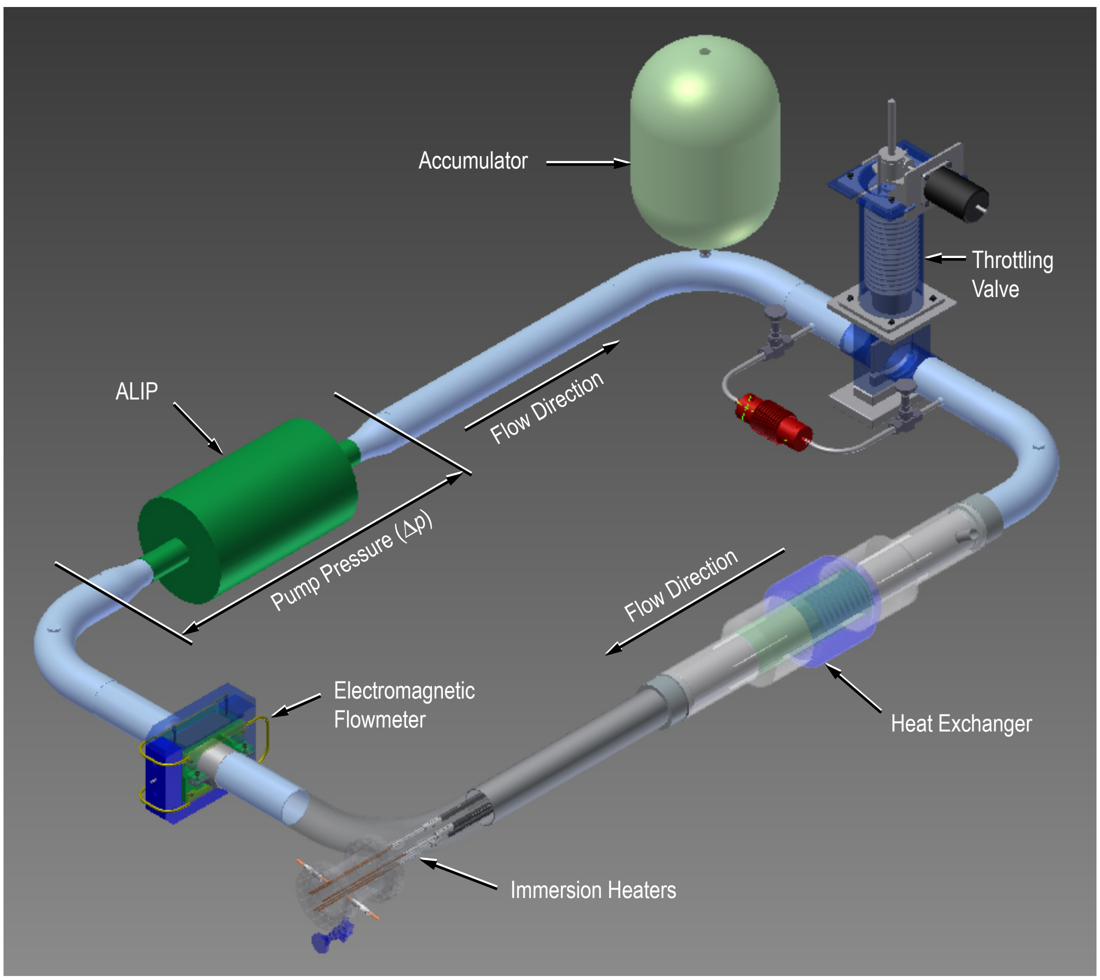

Figure 1. Schematic of the ALIP test circuit configured for TDU ALIP testing.

A plot of pump efficiency as a function of volumetric flow rate, like that shown in figure 2, will exhibit an optimum in efficiency when operating at a constant power (constant power and constant applied voltage are approximately equivalent in an ALIP). This is easily understood in the context of equation (1) and simple concepts of continuity for a closed-loop system. For the bounding case of infinite flow impedance, there is a maximum Δp but $\dot{v}$ is zero, while in the case of no flow impedance in the loop, there is a maximum $\dot{v}$ but zero pressure rise across the pump.

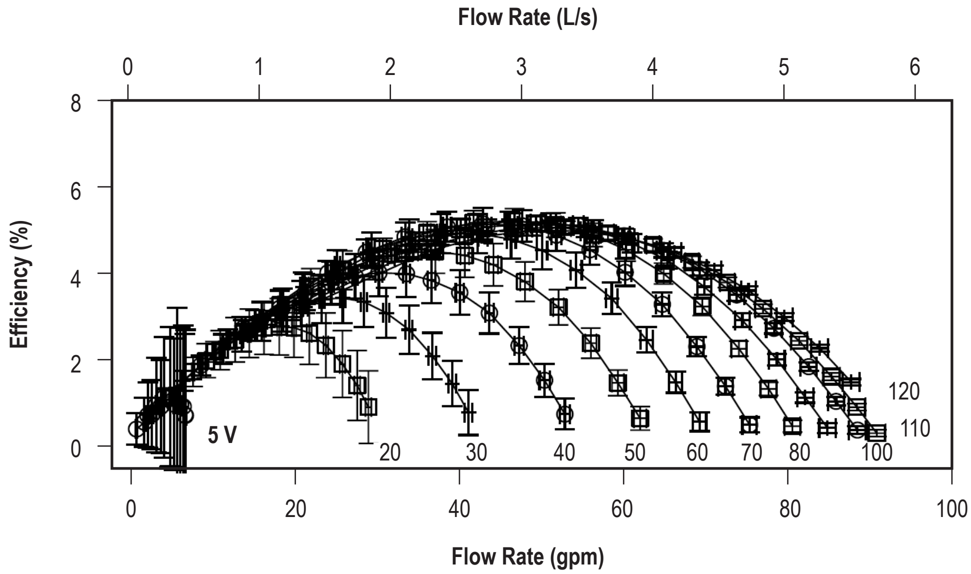

Figure 2. Example efficiency (with error bars) as a function of flow rate and constant pump voltage for NaK at a temperature of 325 ºC and pump frequency of 36 Hz (repeated from ref. 5).

Three-dimensional renderings of two separate ALIP pumps that were tested in the ATC are shown in figure 3. The FSP pump in figure 3(a) was designed for the full-scale 200 kW_t, 40 kW_e fission surface power reference design. The technology demonstration unit (TDU) pump in figure 3(b) was fabricated to support the testing of a TDU, which is a one-quarter scale system (50 kW_t, 10 kW_e) that uses simulated nuclear power to achieve an end-to-end demonstration. In general, an ALIP consists of an annular duct surrounded by a series of solenoidal copper coils positioned inside magnetically-permeable stators elements. An additional magnetically-permeable component is the torpedo, which forms the inner boundary of the annular duct. Three-phase power is applied to the coils, producing an axially-traveling magnetic wave inside the annulus. The high permeability stators concentrate and direct the magnetic field created by the coils radially across the annulus while the torpedo provides the return path for magnetic flux. The axially-traveling radial field induces azimuthal currents in the conducting liquid metal that interact with the magnetic field to yield a net Lorentz body force in the axial direction, pumping the fluid.

(a)

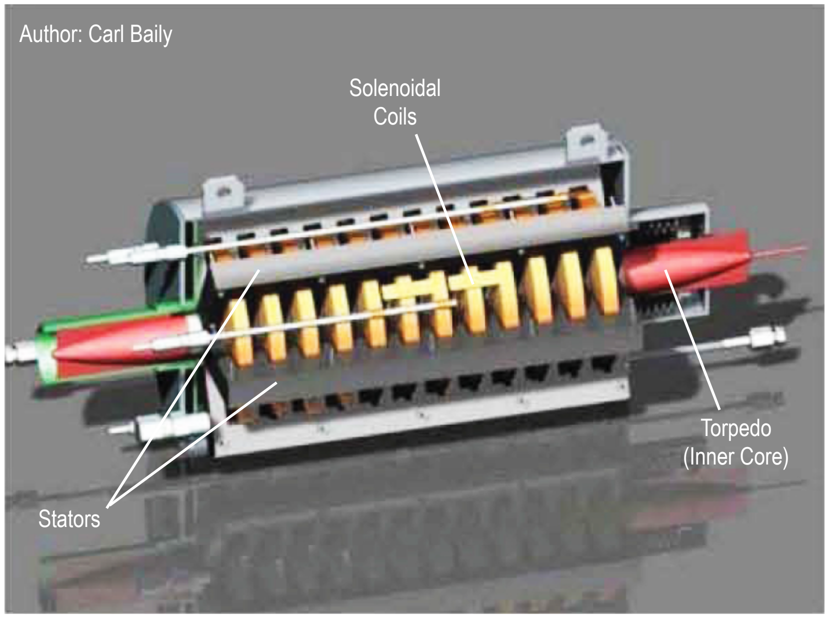

(b)

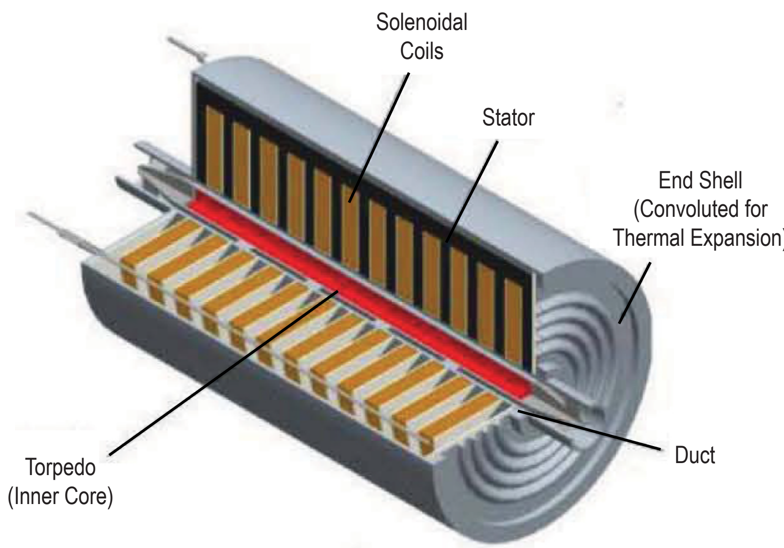

Figure 3. Models: (a) Three-dimensional CAD model of the ALIP tested in reference 5 and (b) cut-away model of the ALIP tested in reference 6; illustrations taken from reference 8.

ALIP experimental data for tests conducted with two separate pumps are found in references 5 and 6. As expected, when efficiency is graphed as a function of volumetric flow rate, these data exhibit an optimum. Other key findings were that the efficiency curves were generally reduced for both higher temperature and at lower power. It was shown that there exists an optimum frequency at which the efficiency of the pump is maximized. This corresponds to the frequency that establishes a traveling magnetic wave velocity that is most conducive to transferring power from the electromagnetic field into the fluid (also known as the condition of minimal 'slip'). The present computational effort aims to produce a model that can replicate these observed phenomena.

3. MULTIPHYSICS MODEL

The ALIP tested in reference 5 was modeled using the commercially available COMSOL Multiphysics version 4.3b. The electromagnetics problem was modeled using the alternating current (AC)/direct current (DC) module while the fluid problem was performed using the computational fluid dynamics (CFD) module. Models were developed separately for each component of the pump, with simplifying assumptions employed to produce an approximate model that could qualitatively reproduce experimental results without requiring intense detailed modeling of any element in the system. The various component models and applied physical properties and boundary conditions are discussed in sections 3.1 through 3.7.

3.1 Domain

The ALIP physical model, shown in figure 4, is representative of the full-sized test apparatus. The model is two-dimensional and axisymmetric, implying no azimuthal variation. For simplicity, the steel casing around the stator and the steel walls of the torpedo were not included in the model. Additionally, the curved, aerodynamic profiles of the front and rear of the torpedo were simplified as conical shaped. The infinite element feature of the program was used for the outermost domain to mathematically simulate a domain that extends indefinitely without the need of unnecessary mesh points.

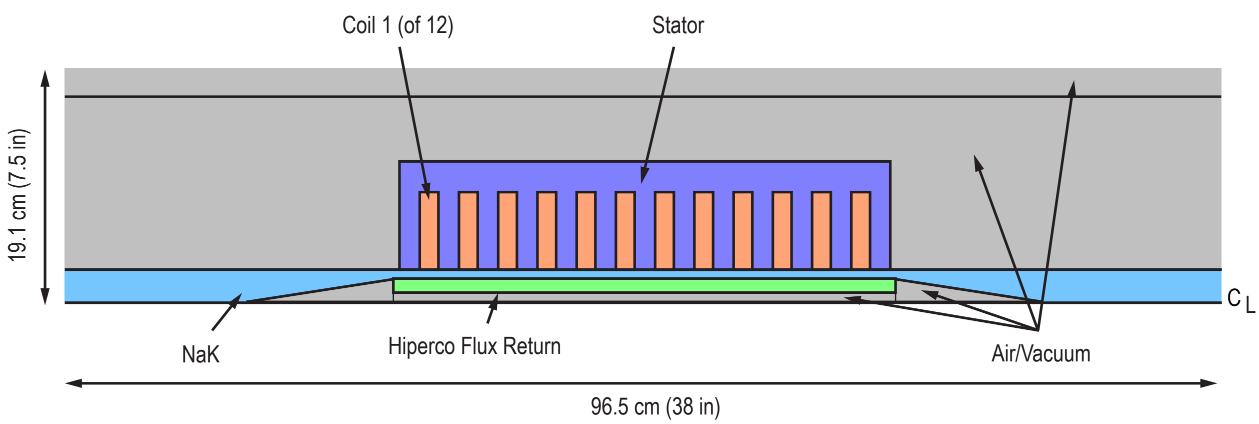

Figure 4. Schematic showing the physical layout of the COMSOL model of ALIP.

3.2 Coils

The ALIP coils were modeled using the multiturn coil domain (MTCD) feature, which implements a homogenized model of a coil using a specified number of wire turns and the cross-sectional area of the wires. The wires used in the experimental ALIP were ribbon-like in shape, measuring 510 µm × 13.6 mm (0.020 × 0.535 in), and were wound 85 times for each coil. The MTCD feature is good for modeling coils with wire diameters that are less than the skin depth of the wire, which is defined as

$$\delta = \sqrt{2/(\omega\mu\sigma)} \ , \tag{2}$$

where ω is the angular frequency of the current, μ is the magnetic permeability of the material, and σ is the electrical conductivity. Using the maximum tested operating frequency of 60 Hz, μ=4π×10^7 H/m, and σ=6×10^7 S/m for copper, the value for the skin depth was calculated to be roughly 8.4 mm (0.33 in). This is significantly larger than the thickness of a single turn of the conductors in the coils, meeting the MTCD sizing requirement. However, while the MTCD feature was used in this particular model, investigation to gain a more complete understanding of this feature's limitations as it applies to ALIP modeling could be a useful avenue of study in future work. (For example, while the depth of one coil winding is 510 µm, the total depth of all 85 turns is over 43 mm and may represent a problem for the MTCD feature.)

The coil domains are further constrained using the Global Equations feature to correctly implement the physical coil configuration of the ALIP (see fig. 5(a)). The Global Equations constraints ensure that the total voltage drop across each leg of the delta configuration sums to the appropriate applied voltage. This yields the effective phase angles for each set of windings based upon the wiring of the pump, as shown in figure 5(b). The coils were assigned the material properties of copper from the COMSOL material database.

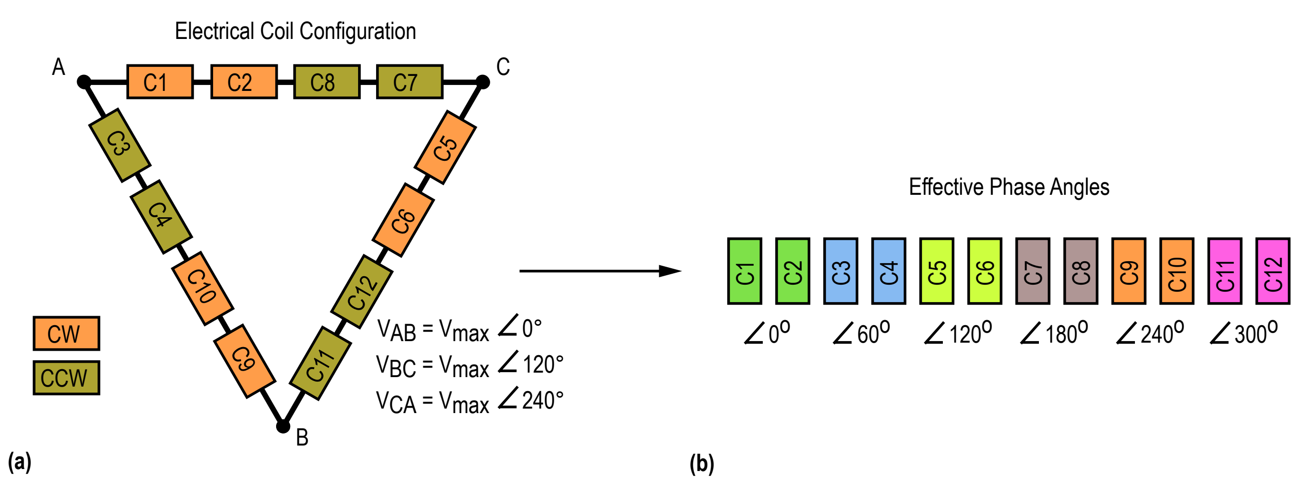

Figure 5. Configurations: (a) Electrical coil configuration and (b) effective phase configuration for the coils in the ALIP.

3.3 Stator

The stator is one of the few components of the ALIP that has significant azimuthal variation. In the tested ALIP, the stators are constructed as six separate finite sections positioned at regular azimuthal intervals around the axis (see fig. 3(a)). Each stator section consists of alternating azimuthal layers (laminates) of steel and an alloy that is itself comprised of 50% Hiperco® 50 and 50% cobalt iron alloy. The alternating azimuthal laminations and the fabrication of the stators as six discreet sections serve to minimize induced circumferential eddy currents. The high magnetic permeability of the stator laminations serve to guide and concentrate the magnetic flux radially into the fluid. As a simplification, and to establish an upper limit on performance, the stator was modeled entirely as Hiperco 50 with zero electrical conductivity, yielding the best magnetic properties while completely suppressing eddy current losses. Future work aimed at understanding how to better model the properties of the three-dimensional stator configuration within a two-dimensional axisymmetric framework could be a useful path to increase the accuracy of the work discussed in this TM.

3.4 Material Properties

The material properties used in the ALIP model are presented in table 1. Included in this table are the associated model domains occupied by each type of material listed. The material properties for copper and air were obtained from the COMSOL program material libraries and the Hiperco 50 values were obtained from the manufacturer, Carpenter Technology Corporation, Reading, PA. The nonlinear *B-H* curve for Hiperco 50 is provided in the appendix. Two entries are listed for Hiperco 50, one with finite electrical conductivity for the flux return in the torpedo, where eddy currents are permitted, and the other with zero conductivity for the stators. This follows from the previous discussion of stator simplification. The material properties of NaK (specifically the eutectic NaK-78 mixture) are summarized in reference 9. The present work only considered an ALIP operating at room temperature conditions (roughly 20 °C, with the corresponding properties for that temperature given in table 1). However, NaK material property curves in reference 9 are given as a function of temperature over the entire ALIP operating envelope (room temperature to roughly 525 °C).

Table 1. Material properties and associated domains used in the ALIP model.

Electromagnetic Properties				
Material	Electrical Conductivity (S/m)	Relative Magnetic Permeability	Relative Electrical Permittivity	Domain
Copper	6.0×10^7	1	1	Coils
Hiperco 50 (with conductivity)	2.5×10^6	Nonlinear *B* vs *H* curve (in the appendix)	1	Flux return
Hiperco 50 (no conductivity)	0	Nonlinear *B* vs *H* curve (in the appendix)	1	Stator
NaK-78 (at 20 °C)	2.38×10^6 (from ref. 9)	1	1	Fluid
Hydrodynamic Properties (From Ref. 9)				
Material	**Density (kg/m^3)**	**Kinematic Viscosity (Pa-s)**	**Thermal Conductivity (J/kg-K)**	**Domain**
NaK-78 (at 20 °C)	875	575	950	Fluid

3.5 Governing Equations

The COMSOL model solves Maxwell's equations within the AC/DC module over all domains while the incompressible, laminar flow, Navier-Stokes equations within the CFD flow solver module are solved within the fluid domain. The fluid equations are affected by the Lorentz body force that arises from the interaction of eddy currents in the flow and the externally-applied magnetic field. The motion of an electrically conductive fluid through a magnetic field also induces a back-electromotive force (EMF) that affects the electromagnetic solution of the problem.

The governing equations are solved using nonlinear segregated solvers, one for each type of problem (electromagnetics and CFD), with Maxwell's equations solved first in the solution process. After this first solution is generated, the model can be solved in time to yield a time-dependent solution of the problem. The model can also be constructed to use a version of Maxwell's equations that assume a cyclic solution. This latter, simplified version of the equation set, also referred to in COMSOL as frequency domain equations, do not permit the incorporation of nonlinear material properties into the model. However, this method can be useful in the initial development and implementation of new model features.

3.6 Boundary Conditions

The fluid domain has no-slip boundary conditions applied to all wall boundaries. A conservation of mass condition is applied to the inlet and outlet of the pump model domain such that the total fluid mass in the domain is conserved. The value of the pressure is pinned to a specified value at one point within the domain and the pressure drop is specified using a periodic flow boundary condition. This allows the user to specify the pressure drop that would occur through the rest of the system as fluid flows through it. In the calculations performed to date, the pressure was pinned to zero at a single corner point in the model. In future work, this can be pinned to values that are close to the measured static pressure in the model. An alternative problem formulation would be to construct a two-dimensional axisymmetric model representing the length of the entire flow loop, where for self-consistency, the pressure at the flow outlet and flow inlet of the simulation domain are equal. It is assumed that there is no magnetic flux out of the computational domain (no flux/zero magnetic potential), with an axis of symmetry condition applied at the centerline.

3.7 Other COMSOL Settings

Many other settings in COMSOL are changed from their default values to achieve convergence. The fluid elements are set to have second-order discretization and the 'consistent stabilization' (numerical dissipation) option was set to 'streamline diffusion.' For the time-dependent solver, the option to exclude algebraic errors from the error estimation was enabled to prevent the inclusion of time-independent errors from the continuity equation. Linear vector elements are used to discretize the magnetic vector potential. This selection can be increased to quadratic elements (recommended) for a more accurate solution to the magnetic field. The Jacobian update option is set so it occurs after every iteration of the electromagnetic solver.

4. MODEL RESULTS

4.1 Axially-Traveling Magnetic Wave

Snapshots of the radial component of the magnetic field located at the midpoint of the annulus as a function of axial location are presented in figure 6. The magnetic field output by the model is presented in figure 6(a) while measured field values taken from reference 5 are given in figure 6(b). The numerical data were obtained from one time-step of a time-varying solution. These data were generated for the case where convecting NaK was in the annulus. The experimentally-acquired data, on the other hand, was obtained at ambient conditions with air filling the annulus. The measurements were performed using a Hall probe that was inserted into the annulus at various axial stations. The model inputs were matched to those used during the experimental measurements and the model was solved using the nonlinear Hiperco 50 properties for the flux return and stators. In these figures, the magnetic wave travels from left to right. The inclusion of NaK within the domain, with its associated Lorentz body force and back EMF, makes it difficult to quantitatively compare these data. In addition, the assumptions that the stator (a) is continuous in the azimuthal direction but permits no flowing circumferential eddy currents and (b) is comprised completely of Hiperco 50, serve to significantly overestimate the calculated radial magnetic field values. While the absolute values of the two curves do not match, likely owing to all the simplifications in the present model, a qualitative comparison between the shapes of the two data sets shows good agreement and suggests that the coil configuration given in figure 5 was correctly implemented in the model.

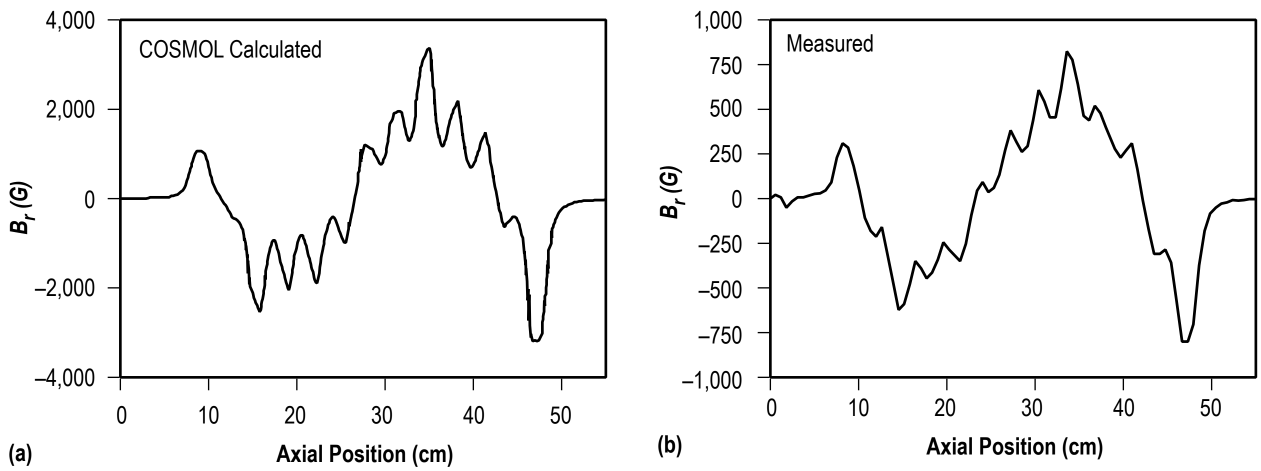

Figure 6. Radial magnetic field B_r as a function of axial position within the pump obtained from (a) the computational COMSOL model and (b) experimental measurements presented in reference 5 (measurements obtained when the annulus was evacuated of NaK).

4.2 Efficiency Curves

A comparison of the pump efficiency as a function of flow rate calculated using the model and experimentally measured and documented in reference 5 are presented in figure 7. The model curve was generated using the frequency domain equations with linear material properties and is therefore not quantitatively comparable to the experimental data since the Hiperco 50 could not experience saturation and because the model was solved at 20 °C where the kinematic viscosity was unrealistically high. Regardless, the existence of a peak in efficiency is promising in terms of providing a check that the physics currently implemented into the model are qualitatively behaving as expected.

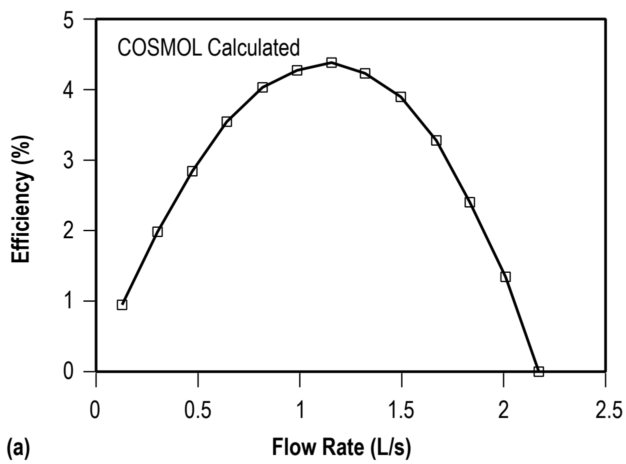

Figure 7. Comparison of (a) modeled and (b) experimental pump efficiency curves for the ALIP of reference 5, operating at three different NaK temperatures (as indicated) with a peak AC voltage of 120 V and frequency of 36 Hz.

4.3 Transient Startup

The average velocity of the fluid as a function of time during a startup transient is presented in figure 8. These data were generated as part of a simplified test case to explore the usage of the model's fully nonlinear, time-dependent solution package. For this case, the pressure at the inlet and exit of the pump were set equal to each other (minimal pump flow impedance). The model was not solved for a long enough time to obtain a steady-state solution, but the solution does appear to be approaching an asymptote. This simulation shows that a fully time-dependent, fully nonlinear solution can be generated for the problem and geometry of interest.

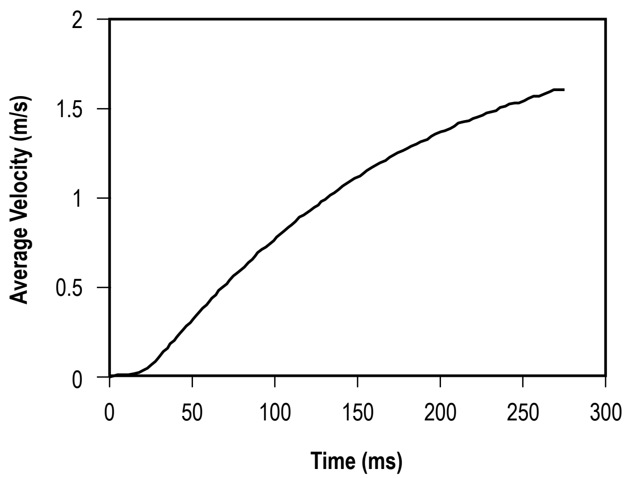

Figure 8. Average calculated velocity of the NaK as a function of time during a startup transient.

5. CONCLUSIONS

The COMSOL Multiphysics model developed in this work, while still incomplete and very simplified, has demonstrated the capability to qualitatively capture many of the experimental data trends observed in testing of an ALIP. The intricate three-phase coil configuration correctly replicates the observed axial-traveling magnetic wave and establishes a net Lorentz body force on the fluid, forcing NaK through the pump. Furthermore, the boundary conditions and input parameters can be easily varied to simulate pump operation over a range of operating conditions, permitting the generation of pump performance curves (efficiency as a function of flow rate). While it may not be desirable to generate fully nonlinear, fully time-dependent solutions of the problem, there are several less accurate or simplified methods with which the model can be solved that can be used to provide a rapid check on the solution methodology being employed. Though additional validation is still required, a simplified solution method and the approximate model presented in this TM may be very useful in developing a systematic understanding of measured ALIP performance scaling as a function of different physically controllable parameters.

APPENDIX—HIPERCO 50 *B-H* DATA

The nonlinear *B-H* curve for Hiperco 50, as provided by the manufacturer, Carpenter Technology Corporation, Reading, PA, is presented in figure 9.

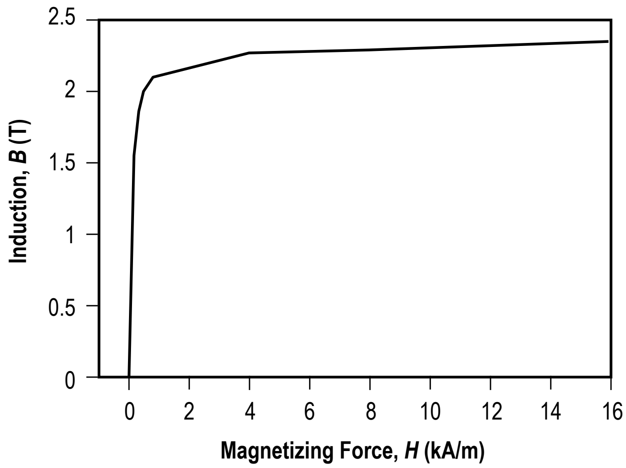

Figure 9. Hiperco 50 *B-H* curve data (taken for material strips with a heat treatment of 871 ºC (1,600 ºF)).

REFERENCES

1. Nainiger, J.: "Affordable Fission Surface Power System Study Final Report," NASA Exploration Systems Mission Directorate Report, Glenn Research Center, Cleveland, OH, October 2007.

2. Mason, L.S.: "A Comparison of Fission Power System Options for Lunar and Mars Surface Applications," NASA/TM—2006–214120, Glenn Research Center, Cleveland, OH, 21 pp., February 2006.

3. Mason, L.S.: "A Practical Approach to Starting Fission Surface Power Development," NASA/TM—2006–214366, Glenn Research Center, Cleveland, OH, 11 pp., July 2006.

4. Mason, L.S.; Poston, D.; and Qualls, L.: "System Concepts for Affordable Fission Surface Power," NASA/TM—2008–215166, Glenn Research Center, Cleveland, OH, 17 pp., January 2008.

5. Polzin, K.A.; Pearson, J.B.; Schoenfeld, M.P.; et al.: "Performance Testing of a Prototypic Annular Linear Induction Pump for Fission Surface Power," NASA/TP—2010–216430, Marshall Space Flight Center, Huntsville, AL, 118 pp., May 2010.

6. Polzin, K.A.; Pearson, J.B.; Webster, K.; et al.: "Testing of an Annular Linear Induction Pump for Fission Surface Power Technology Demonstration Unit," NASA/TP—2013–217487, Marshall Space Flight Center, Huntsville, AL, 36 pp., August 2013.

7. Goldsteins, L.; Buligins, L.; Fautrelle, Y.; et al.: "Numerical Quasi Stationary and Transient Analysis of Annular Linear Electromagnetic Induction Pump," Proceedings of the 2013 COMSOL Conference, Rotterdam, The Netherlands, October 23–25, 2013.

8. Maidana, C.O.; Werner, J.E.; and Wachs, D.M.: "Design of an Annular Linear Induction Pump for Nuclear Space Applications," Paper No. 3236, Proceedings of Nuclear and Emerging Technologies for Space 2011, Albuquerque, NM, February 7–10, 2011.

9. Polzin, K.A.: "Liquid-Metal Pump Technologies for Nuclear Surface Power," NASA/TM—2007–214851, Marshall Space Flight Center, Huntsville, AL, 36 pp., March 2007.

REPORT DOCUMENTATION PAGE

Form Approved
OMB No. 0704-0188

1. REPORT DATE *(DD-MM-YYYY)*
01–03–2014

2. REPORT TYPE
Technical Memorandum

3. DATES COVERED *(From - To)*

4. TITLE AND SUBTITLE
Multiphysics Modeling of an Annular Linear Induction Pump With Applications to Space Nuclear Power Systems

5a. CONTRACT NUMBER

5b. GRANT NUMBER

5c. PROGRAM ELEMENT NUMBER

6. AUTHOR(S)
J. Kilbane and K.A. Polzin

5d. PROJECT NUMBER

5e. TASK NUMBER

5f. WORK UNIT NUMBER

7. PERFORMING ORGANIZATION NAME(S) AND ADDRESS(ES)
George C. Marshall Space Flight Center
Huntsville, AL 35812

8. PERFORMING ORGANIZATION REPORT NUMBER
M–1377

9. SPONSORING/MONITORING AGENCY NAME(S) AND ADDRESS(ES)
National Aeronautics and Space Administration
Washington, DC 20546–0001

10. SPONSORING/MONITOR'S ACRONYM(S)
NASA

11. SPONSORING/MONITORING REPORT NUMBER
NASA/TM—2014–217501

12. DISTRIBUTION/AVAILABILITY STATEMENT
Unclassified-Unlimited
Subject Category 20
Availability: NASA STI Information Desk (757–864–9658)

13. SUPPLEMENTARY NOTES
Prepared by the Propulsion Systems Department, Engineering Directorate

14. ABSTRACT
An annular linear induction pump (ALIP) that could be used for circulating liquid-metal coolant in a fission surface power reactor system is modeled in the present work using the computational COMSOL Multiphysics package. The pump is modeled using a two-dimensional, axisymmetric geometry and solved under conditions similar to those used during experimental pump testing. Real, nonlinear, temperature-dependent material properties can be incorporated into the model for both the electrically-conducting working fluid in the pump (NaK-78) and structural components of the pump. The intricate three-phase coil configuration of the pump is implemented in the model to produce an axially-traveling magnetic wave that is qualitatively similar to the measured magnetic wave. The model qualitatively captures the expected feature of a peak in efficiency as a function of flow rate.

15. SUBJECT TERMS
ALIP, annular linear induction pump, multiphysics modeling, space nuclear power, nonlinear modeling, electromagnetic pump

16. SECURITY CLASSIFICATION OF: a. REPORT	b. ABSTRACT	c. THIS PAGE	17. LIMITATION OF ABSTRACT	18. NUMBER OF PAGES	19a. NAME OF RESPONSIBLE PERSON
U	U	U	UU	28	STI Help Desk at email: help@sti.nasa.gov
					19b. TELEPHONE NUMBER *(Include area code)* STI Help Desk at: 757–864–9658

National Aeronautics and
Space Administration
IS20
George C. Marshall Space Flight Center
Huntsville, Alabama 35812